JSEE Vol. 23, No. 1, 2021 DOI: 10.48303/jsee.2022.1982993.1041

Research Paper

Inelastic Response Spectrum for Foreshock-Mainshock-Aftershock Sequences

Morteza Bastami[1*] and Mohammad Jonaidi[2]

1. Associate Professor, Structural Engineering Research Center, International Institute of Earthquake Engineering and Seismology (IIEES), Tehran, Iran,
*Corresponding Author; email: m.bastami@iiees.ac.ir
2. M.Sc. Student, University of Kurdistan, Sanandaj, Iran

Received: 17/12/2022
Revised: 26/12/2022
Accepted: 28/12/2022

ABSTRACT

The effect of aftershocks on structures is not usually considered in seismic design codes. In addition to mainshock events, aftershocks can cause major damage to structures, especially to mainshock-damaged structures. Analysis of the characteristics of the mainshock, foreshocks, and aftershocks reveal differences in the ground motion parameters. Structures may undergo a variety of seismic waves with different characteristics that can increase the chance of seismic amplification. The present study examined the effects of aftershock as well as foreshocks events on the response of single degree-of-freedom (SDOF) systems with nonlinear behavior. This allowed inclusion of possible differences during calculation of the response spectrum for cases having foreshock and aftershock effects and those excluding these effects. To this end, 38 mainshocks from different seismic regions with moment magnitudes (M_w) greater than 3.5 were used. More than 168 records from mainshock, aftershock, and foreshock events were applied to evaluate the effects of aftershocks and foreshocks on the response spectrum. The parameters of post-yield stiffness ratio (hardening and softening), ductility factor, period, and site classification were taken into account during 121,000 nonlinear analyses on 60 SDOF models. The results show that the aftershocks as well as foreshocks have a significant effect on the response spectrum, increasing the structural response. Consequently, the effect of aftershocks must be considered in the development of design spectra in seismic codes and guidelines.

Keywords:
Aftershock; Foreshock; Response spectrum; Single-degree-of-freedom structure; Nonlinear response; Earthquake

1. Introduction

Although earthquakes are followed by many aftershocks, the effects of these aftershocks are not considered in seismic design codes. The importance of aftershocks has been observed in the past earthquakes such as the 1994 Northridge (USA), 1997 Umbria-Marche (Italy), 2008 Wenchuan (China), 2010 Darfield (New Zealand), 2011 Christchurch (New Zealand), 2011 Van (Turkey), 2011 Great Tohoku (Japan), 2012 Emilia (Italy), and 2015 Nepal earthquakes. Aftershocks have repercussions for structural performance and can repeat many times. Aftershocks increase fear and concern of residents in addition to disruption of relief and rescue operations if buildings have been damaged or destroyed in earthquake-stricken areas.

The 2011 Great Tohoku earthquake with M_w of 9.0 was followed by many aftershocks and revealed that visually-stable structures are more vulnerable to severe damage and collapse during an aftershock. Mainshock-damaged buildings are more prone to accumulated damage from aftershocks because of their reduced structural capacity [1]. To evaluate the realistic behavior of structures experiencing earthquakes, multiple earthquakes comprising a mainshock and aftershocks should be considered as a single seismic loading. The structures must be analyzed under the mainshock-aftershock sequences to consider the effects of aftershocks.

Few studies have been carried out on the seismic performance of structures under mainshock-aftershock sequences, although the importance of aftershocks has been observed in previous earthquakes. The present study reviews earlier research on the effect of aftershocks on structures.

Mahin [2] showed that structural damage could increase with the experience of aftershocks in which the accumulation of damage can cause the collapse of the structure. Sunasaka and Kiremidjian [3] calculated the damage to structures caused by mainshock-aftershock earthquake sequences using a new method. Their findings showed that cumulative damage of the mainshock and aftershock may be significantly different from the effect of the mainshock only.

Aschheim and Black [4] proposed a hysteretic pinching model of single degree-of-freedom (SDOF) systems for concrete and masonry wall buildings. The effect of prior earthquake damage on peak displacement responses was evaluated in their study. The strength of the oscillator, period of vibration and extent of prior damage were included in the SDOF system. The ground motion used (18 pairs of repeated ground motion) for analysis show differences in frequency content, duration and the presence or absence of near-fault directivity effects. The only prior damage considered was a decrease in initial stiffness that could cause underestimation of overall deformation in real situations. Gallagher et al. [5] investigated damaged structures during aftershocks following major earthquakes in the USA and showed that considerable damage to buildings could occur.

The non-linear response of SDOF systems under repeated ground motions was studied by Amadio et al. [6] using different values for damping ratio, hysteretic models and ductility factors. The result of loading from a mainshock only, one mainshock and one aftershock, one mainshock with two aftershocks events showed that multiple earthquakes change the response spectrum and that differences can be reduced by increasing the ductility factor. Their analysis on a moment-resisting steel frame demonstrated a diminution of the behavior factor under multiple earthquakes. They recommended supplementary analysis, particularly for structures with low ductility.

A reduction of the behavior factor was proposed by Fragiacomo et al. [7] based on the response of steel frames, including moment-resistant frames with rigid and semi-rigid joints and a braced steel frame. Luco et al. [8] determined the residual capacity of damaged structures under aftershocks using nonlinear dynamic and static-pushover analysis and compared the results of these two methods. The results showed that the static-pushover approach can be unreliable for estimation of residual capacity.

Iancovici and Georgiana [9] investigated the effect of repeated ground motion on the behavior of and parameters for inelastic energy dissipation of a structure. The residual capacity of low-rise reinforced concrete (RC) structures damaged during earthquakes based on the ratio of residual seismic capacity to initial capacity was estimated by Maeda and Kang [10] using a new method.

Hatzigeorgiou and Beskos [11] calculated the inelastic displacement ratio of a structure subject to repeated earthquakes. They showed that multiple earthquakes have a considerable effect on this ratio. Their study used the parameters of site classification, viscous damping ratio, post-yield stiffness ratio, and behavior factor for analysis considering four types of seismic loading: only mainshock (case 1), mainshock with one aftershock (case 2), mainshock with three aftershocks (case 3), and mainshock with aftershocks and foreshocks (case 4). Hatzigeorgiou and Liolios [12] analyzed eight low- and mid-rise RC frames subject to 45 repeated ground motions that included real and artificial sequences. They demonstrated that the sequence of the ground motions has a significant effect on the response and it is essential to re-evaluate seismic design procedures.

Moustafa and Takewaki [13] found that aftershocks can cause greater damage to a structure than the mainshock because of the accumulation of inelastic deformation. Other studies have evaluated damage indices for structures under mainshock-aftershock sequences [14-15]. Jeon [16] developed a probabilistic procedure to show the vulnerability of mainshock-damaged structures in response to aftershocks. Iervolino et al. [17] obtained closed-form estimates for aftershock reliability of elastic perfectly-plastic damage accumulation systems. Zhai et al. [18] showed that aftershocks have a significant effect on destruction of structures if the ratio of aftershock peak ground acceleration (PGA) to mainshock PGA is > 0.5.

The vulnerability of RC frames to aftershocks was investigated by Raghunandan et al. [19] using incremental dynamic analysis. They showed that if the structure is not severely damaged in the mainshock then the aftershocks will not strongly contribute to collapse capacity. If the building is extensively damaged in the mainshock, there is a considerable decrease in collapse capacity under aftershocks. Abdollahzadeh et al. [20] developed a new design method known as performance-based plastic design (PBPD) has been utilized instead of conventional elastic design (ED) for steel moment frames, which considers nonlinear behavior of structures directly in the design process. Result of time-history analysis shows that drift increase due to the aftershock for ED-frame is more than PBPD-frame. In addition, plastic hinge and hysteretic energy distributions for PBPD-frame when subjected to mainshock-aftershock sequence is more desirable than ED-frame.

The present study examined the effects of both foreshocks and aftershocks on the response spectrum in the design of structures. This has not been well-studied in the literature. Records from 38 mainshocks from Japan, Iran, the US, and Europe with moment magnitudes of > 4 were chosen. The real sequences were constructed from the National Research Institute for Earthquake Science and Disaster Prevention (K-NET) for Japanese earthquakes, Pacific Earthquake Engineering Research (PEER [21]) for US and European earthquakes and International Institute of Earthquake Engineering and Seismology (IIEES) [22] for Iranian earthquakes. More than 168 acceleration time series from these events, including foreshocks, mainshocks and aftershocks, were applied to SDOF systems to obtain a design acceleration spectrum. The influence of structure vibration period, ductility factor, soil type, and post-yield stiffness ratio (hardening and softening) was considered and discussed.

2. Methodology

To design new structures or seismically evaluate existing structures, it is necessary to use the design spectra. The effects of aftershocks have been ignored in the development of design spectra; however, the importance of aftershocks has been proven in literature reviews and through observations. It appears that the effect of aftershocks should be considered during the development of design spectra for a seismic design that is safe under mainshock-aftershock sequences. The response spectrum under the effect of aftershocks can be calculated by applying aftershocks to a mainshock-damaged structure experiencing permanent and plastic deformation. This response spectrum can be compared for multiple earthquakes or only one mainshock.

Nonlinear analysis requires the use of an elasto-plastic SDOF system with hardening or softening and assumes viscous damping (Figure 1). The dynamic equilibrium equation of a SDOF system is:

$$m\ddot{u} + c\dot{u} + k_t u = -ma_g \quad (1)$$

where m is the mass, u the relative displacement, c the damping coefficient, k_t the tangent stiffness, and a_g the ground motion acceleration. The indi-

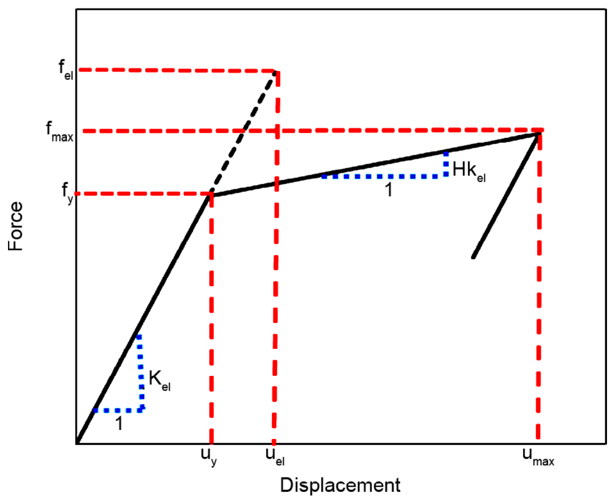

Figure 1. Bilinear elastoplastic model of SDOF models.

cators over u denote time derivatives. The required yield force for a system with adequate ductility is denoted by f_y and the maximum force corresponding to linear elastic system is denoted by f_{el} (Figure 1); thus, the force reduction factor (R) can be defined as $R = f_{el}/f_y$, yield force f_y can be expressed in terms of yield displacement u_y and elastic stiffness k_{el} as $f_y = k_{el}.u_y$. Moreover, the ductility factor is defined as the ratio of maximum displacement (u_{max}) to yield displacement (u_y). Strain hardening or softening takes place above the yielding threshold. The slope of the second branch of the force-displacement relationship (Figure 1) is known as tangent stiffness ($k_t = H.k_{el}$).

The nonlinear response spectrum with constant ductility was calculated for five cases: mainshock only (case 1), mainshock plus first aftershock (case 2), mainshock plus all aftershocks (case 3), mainshock plus foreshocks (case 4), and mainshock plus aftershocks and foreshocks (case 5). The spectral periods for calculation of the responses of the SDOF system were all 0-3 s.

The Newmark method was used for nonlinear analysis assuming $\beta = 0.25$ and $\gamma = 0.5$ in which the stiffness of the system changes according to the Newton-Raphson numerical method in each step [23]. Open System for Earthquake Engineering Simulation (OPENSEES [24]) software was used for nonlinear analysis.

3. Database and Processing

About 38 mainshock earthquakes are selected from Iran Strong Motion Network (ISMN) (http://site.bhrc.ac.ir/portal/english/Home.aspx) [25], NIED Strong-motion seismograph networks, Japan (http://www.kyoshin.bosai.go.jp/) [26] and PEER Ground Motion Database, USA (http://ngawest2.berkeley. edu) [21]. A total of 168 accelerograms were collected and included mainshocks, aftershocks, and fore-shocks (Tables A1 and A2 in Appendix A). The records were classified according to International Building Code (IBC) [27] regulations into two site conditions based on average shear velocity at a depth of 30 m (V_{s30}) for rock (V_{s30} > 365 m/s) and soil (V_{s30} < 365 m/s). There were 19 rock and 20 soil sites. The mainshock of an earthquake and its aftershocks and foreshocks were all recorded at one station.

The accelerograms indicate that there was no limit to the number of aftershocks recorded for a one month time interval after the mainshock. Some earthquakes were followed by one aftershock and others by up to nine aftershocks. Records with a PGA of less than 0.05 g were excluded from the analysis. The characteristics collected from the accelerograms were station name, date and time of occurrence, PGA, magnitude, focal depth, site condition, dominant frequency and significant duration.

Table (1) gives an example of the great Tohoku March 11, 2011 earthquake recorded at station MYG004. The characteristics of all records are shown in Appendix A (Table A1). All earthquake magnitudes in Table A1 have been converted to moment magnitude scale according to method proposed by Boore and Joyner [28]. Significant duration is defined as the interval between times at specific Arias intensity values. The onset of duration is considered when the Arias intensity is about 5% of the total Arias intensity. The end-point is either at 75% [29] or 95% [30] of the total Arias intensity.

All acceleration time series of seismic sequences were normalized using the PGA of the mainshock

Table 1. Mainshock with aftershocks for Great Tohoku, Japan earthquake (Mar 11, 2011).

Event	Date	Time	M	Depth (km)	PGA (g)	Fourier Amplitude (m/s)	Max Frequency (Hz)	t_{5-95} (s)	t_{5-75} (s)	Site Class
Mainshock	11 Mar 2011	14:46	9	24	3.12	26.821	6	80.86	52.16	Rock
Aftershock	11 Mar 2011	15:09	7.4	32	0.112	0.961	6.33	218.3	179	Rock
Aftershock	11 Mar 2011	15:26	7.5	34	0.096	1.167	7.86	46.65	31.12	Rock
Aftershock	11 Mar 2011	16:29	6.5	36	0.24	1.697	6.07	24.18	16.14	Rock
Aftershock	11 Mar 2011	20:37	6.7	24	0.109	0.903	7.68	160.9	13.56	Rock
Aftershock	24 Mar 2011	17:21	6.2	34	0.176	0.912	6.47	12.2	3.46	Rock
Aftershock	28 Mar 2011	07:24	6.5	31	0.122	0.657	6.23	22.93	8.77	Rock
Aftershock	02 Apr 2011	13:08	5.2	42	0.125	0.481	8.81	7.38	2.11	Rock
Aftershock	07 Apr 2011	23:32	7.1	66	1.211	11.085	6	15.75	7.67	Rock
Aftershock	09 Apr 2011	18:42	5.4	58	0.187	0.863	9.48	4.91	1.01	Rock

to allow comparison. Normalizing allows evaluation and comparison of the responses of the seismic sequence with the mainshock. For a set of earthquakes in which the PGA of the aftershocks is less than the mainshock, maximum acceleration is equivalent to 1 after normalization (Figure 2). For a set of earthquakes in which the PGA of aftershocks is greater than the mainshock, maximum acceleration is greater than 1 after normalization (Figure 3).

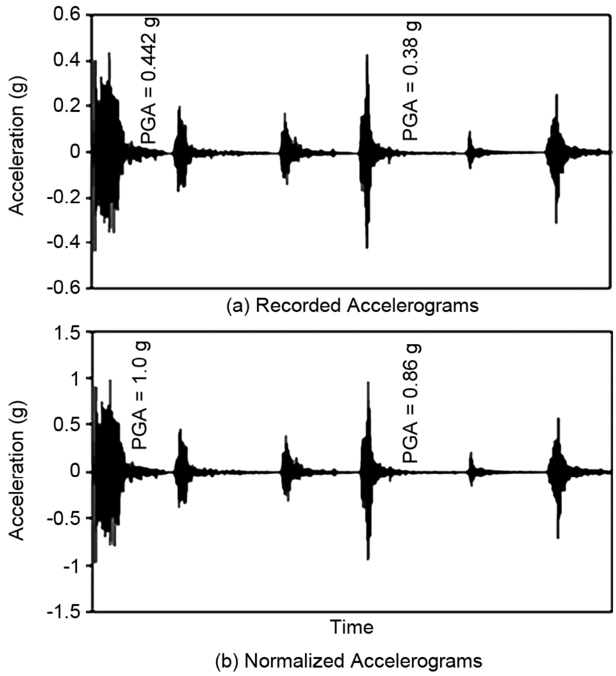

Figure 2. Accelerograms for Mammoth Lakes earthquake and its aftershocks (May 25, 1980).

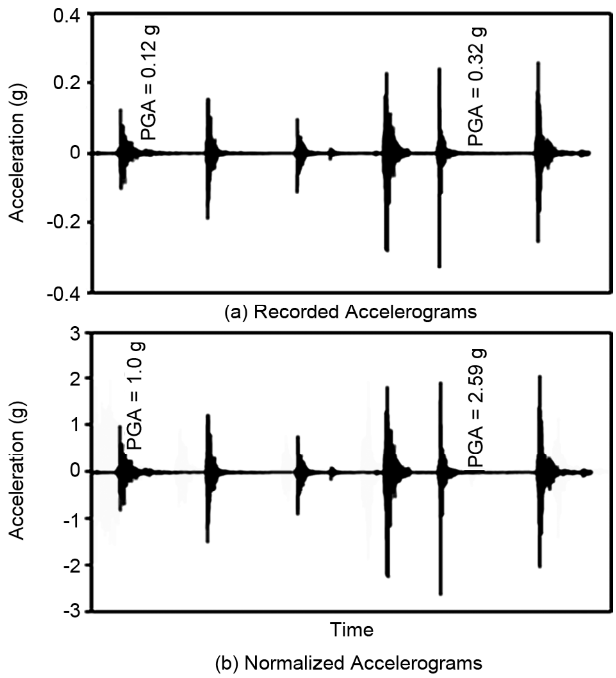

Figure 3. Accelerograms of a Japan earthquake and its aftershocks (August 3, 2000).

Five combinations of seismic sequences (case 1, case 2, case 3, case 4, and case 5) were used to study the effects of different parameters on the response spectrum, as shown in Figure (4).

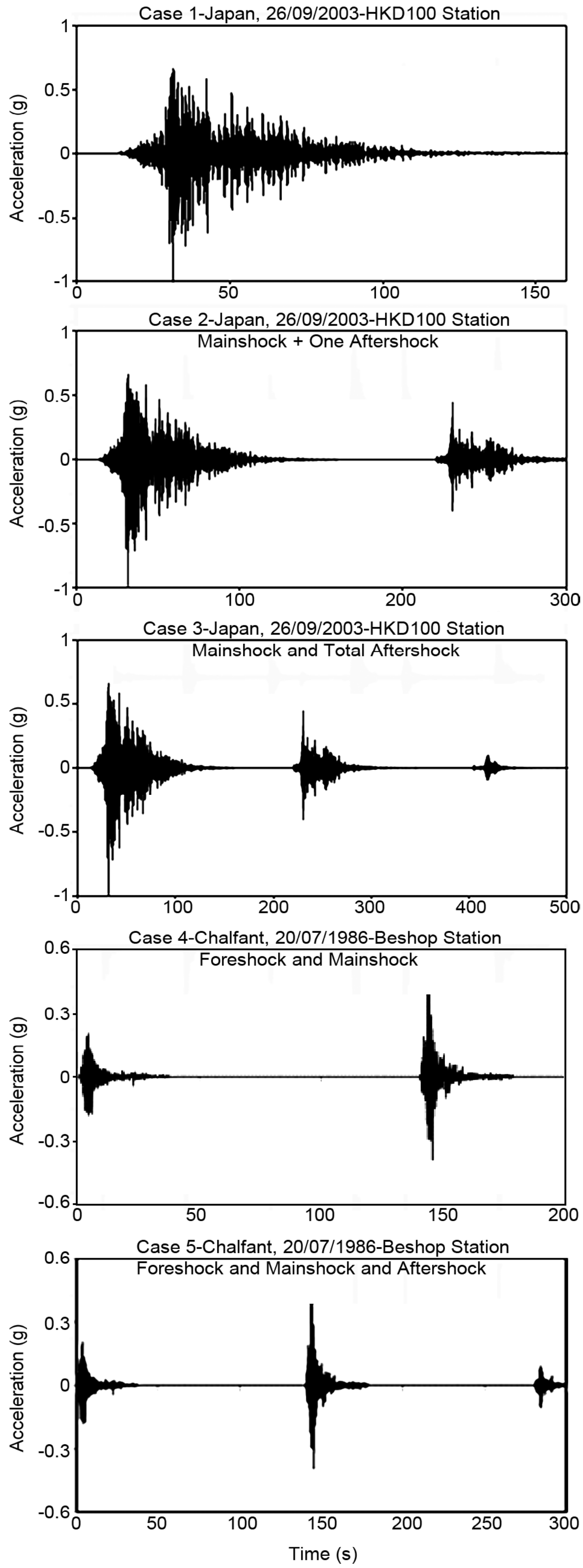

Figure 4. Seismic sequences for analysis (cases 1, 2, 3, 4 and 5) assuming a time gap of 100 sec.

The time interval between seismic sequences was about 100 s, as shown in Figure (5) and allows examination of the effects of free vibration in the SDOF models. The response spectrum for the SDOF systems at ξ = 5% under multiple earthquakes are shown in Table (1) with ductility factors of 1, 2, 4, 8. These are plotted in Figure (6) in terms of Sa/g and natural period.

For each earthquake in nonlinear analysis, SDOF structures with periods of up to 3 s (60 SDOF structures) and four ductility factors (1, 2, 4, and 8) were considered. A total of 120960 nonlinear analyses are conducted for the earthquake records: (38 mainshocks × cases 1, 2, 3 of repeated ground motion + 6 mainshocks × cases 4 and 5 of repeated ground motion) × (60 SDOF structures) × (one viscous damping ratio) × (H = -0.05, -0.03, 0.03, 0.05) × (ductility factors of 1, 2, 4, and 8).

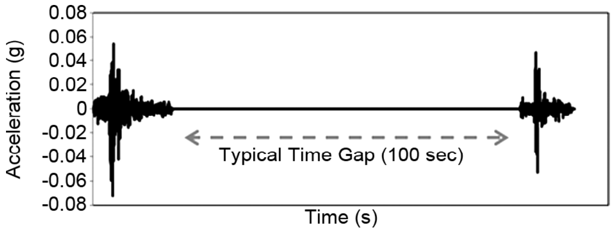

Figure 5. Accelerogram of Livermore earthquake and its aftershock (January 24, 1980) at M_w = 5.8.

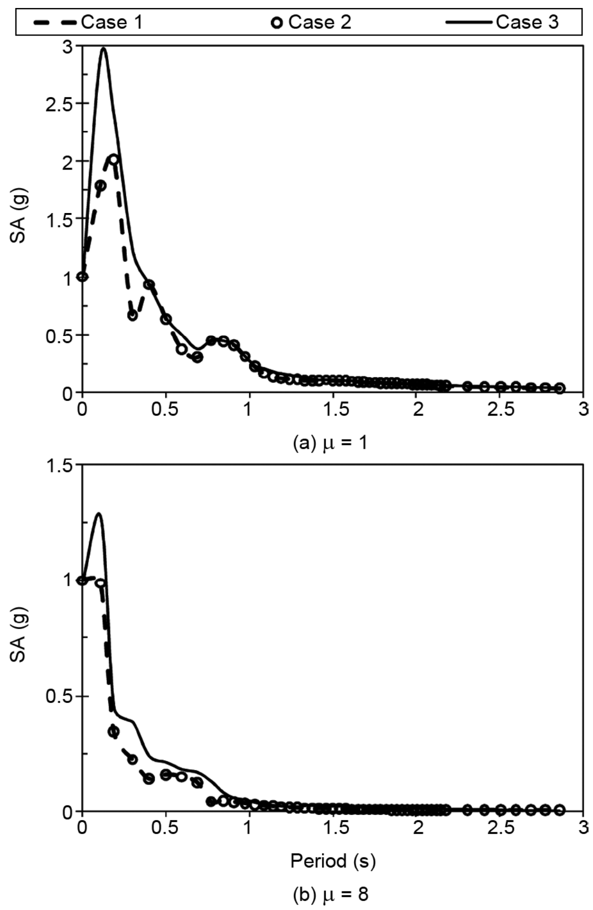

Figure 6. Response spectrum of Japan earthquake (October 23, 2004) for ductility factors of (a) 1.0 and (b) 8.0 at rock sites assuming H = -0.03 and ξ = 5%.

4. Results and Discussion

4.1. Aftershock (Cases 1, 2 and 3) and Soil Site Conditions

In Figure (7), where the ductility factor is assumed to be 1 (μ = 1), the response spectrum for case 3 was of greater spectral amplitude than for cases 1 and 2, and the importance of considering the effects of aftershocks is demonstrated. The behavior of the seismic sequences (cases 1, 2 and 3) are quite different for spectral amplitudes of periods of up to 1 s at soil sites. For example, the differences between cases 1 and 2 were negligible and the peak value at T = 0.2 s was amplified about 11% in case 2. The peak value in case 3 increased about 47% over case 1, confirming the effects of the aftershocks. The aftershocks had a significant effect on response spectrum. This effect must be considered during the development of the design spectrum. Seismic codes and guidelines currently ignore this effect; the design spectrum is underestimated in existing seismic codes because the effect of aftershocks is not considered.

4.2. Effect of Post-Yield Stiffness Ratio

Figure (8) assumes ductility factors of 4 and 8 and shows that differences of spectral amplitude for different seismic sequences (cases 1, 2 and 3) is not highly dependent on the ductility factor. The greatest difference occurred between cases 3 and

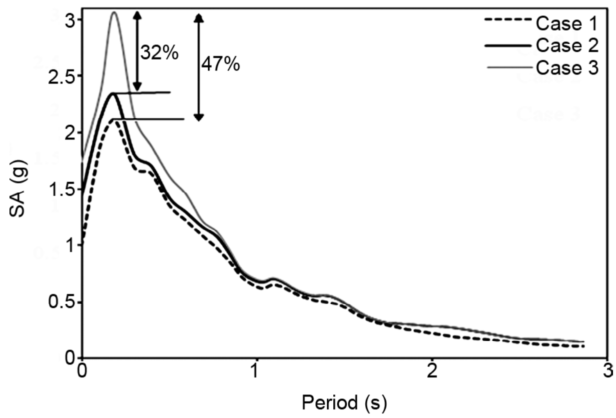

Figure 7. Effects of cases on response spectrum at soil sites assuming μ = 1, ξ = 5%, and H = 0.03.

1 for a period of 0.2 s. The ductility factor for case 3 was about 18% at a $\mu = 4$ and for case one was about 18.5% at $\mu = 8$. The responses for case 2 with respect to case 1 did not change noticeably.

The ratios of spectral responses for cases 2 and 3 to case 1 are plotted in Figure (9). The value for R_n / R_1 denotes the spectral ratio of case n to case 1. Differences between the responses of case 1 and cases 2 and 3 for all periods are evident (the spectral ratio is not equivalent to one). Differences between case 2 and case 3 at $\mu = 1$ and $\mu = 8$ are for periods of up to 1 s.

The effect of post-yield stiffness ratio on the response spectrum is shown in Figure (10) for cases 1 and 3 assuming $\mu = 8$ at soil sites and post-yield stiffness ratios of -0.05, -0.03, 0.03, and 0.05.

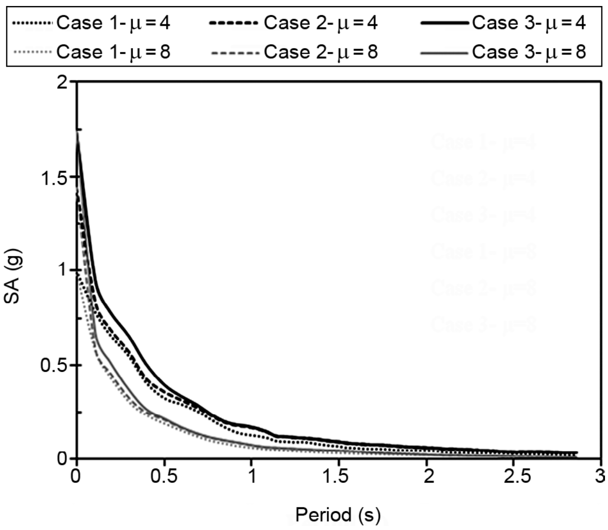

Figure 8. Effect of case ductility factors (μ = 4 and 8), ξ = 5% and H = 0.03 on response spectrum at soil sites.

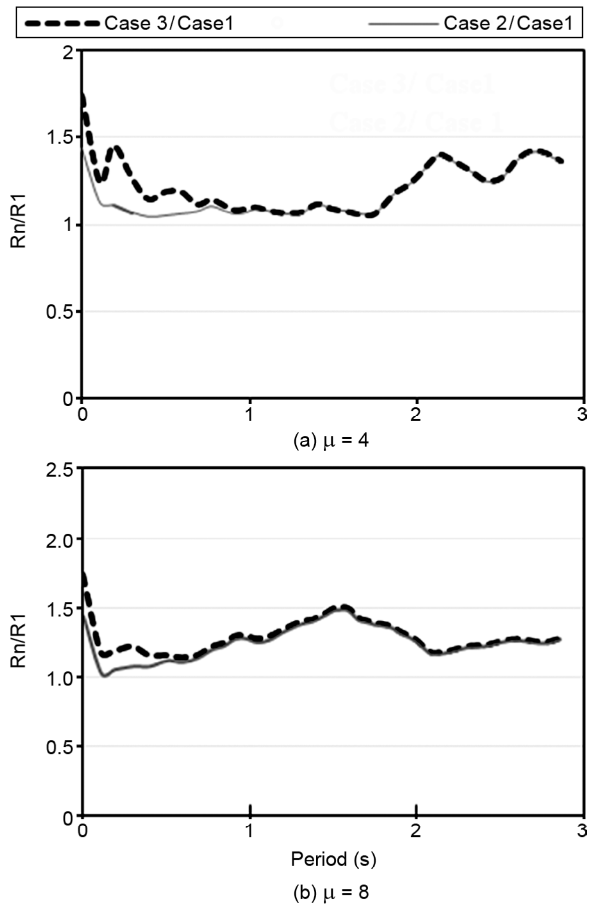

Figure 9. Effects of cases on response spectrum at soil sites assuming ξ = 5%, H = 0.03 and (a) μ = 4 (left) and (b) μ = 8.

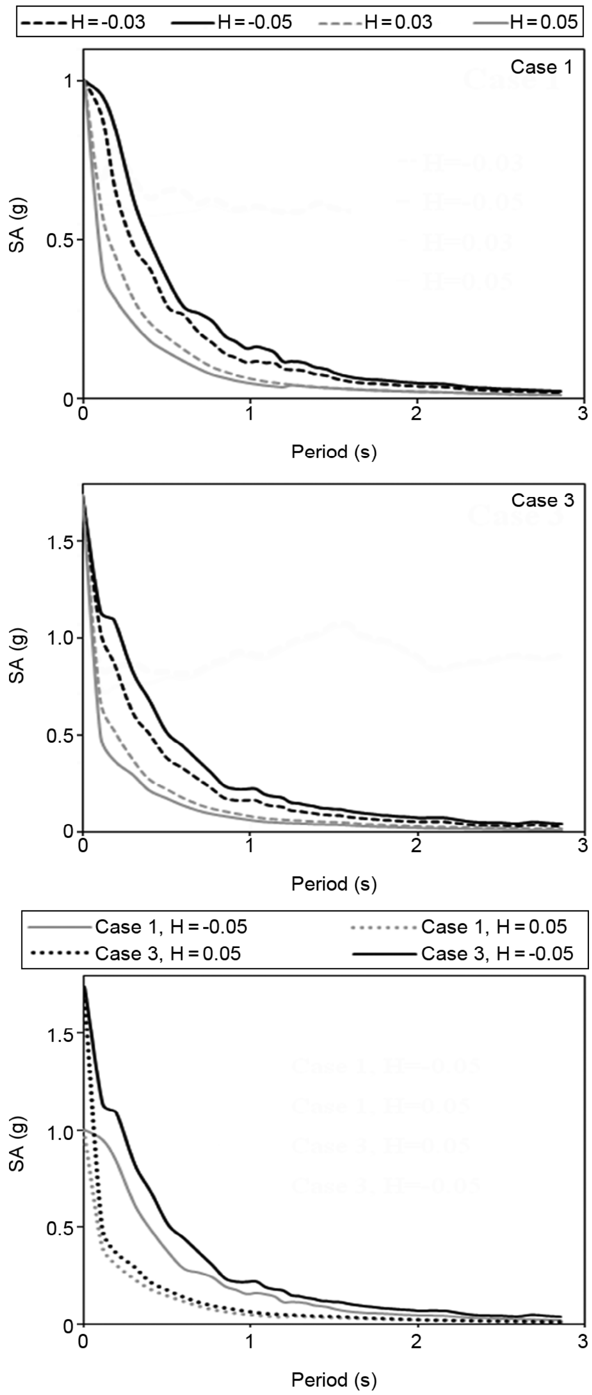

Figure 10. Effect of case and post-yield stiffness ratio on response spectrum at soil sites assuming μ = 8 and ξ = 5%.

The ratio of spectral amplitude for H = 0.03 and 0.05 are compared in Figure (11). Figure (12) is similar to Figure (8), but the post-yield stiffness ratios are 0.03 to -0.03. There is no important change in spectrum for case 2 in comparison with case 1 for the periods of up to 1 s. The difference between cases 2 and 3 for a period of 0.2 s is about 6% for μ = 8 and 7.6% for μ = 4. These differences at the same period will be about 32% for μ = 4 and 34% for μ = 8 for cases 1 and 3.

It can be concluded that the post-yield stiffness ratio affects the responses. Changes in the response spectrum for different seismic sequences (soil sites) increased from 18.5% to 34% as the post-yield stiffness ratios increased. Figure (12) illustrates this effect for cases 2 and 3; the responses at a post-yield stiffness ratio of -0.03 was greater than of 0.03 compared to case 1. Figure (13) shows the effects of case and post-yield stiffness ratio of the response spectrum at soil sites assuming H = -0.03 and ζ = 5% for μ = 4. *Rn* is the response value for cases 2 and 3 and R1 is the response value for case 1.

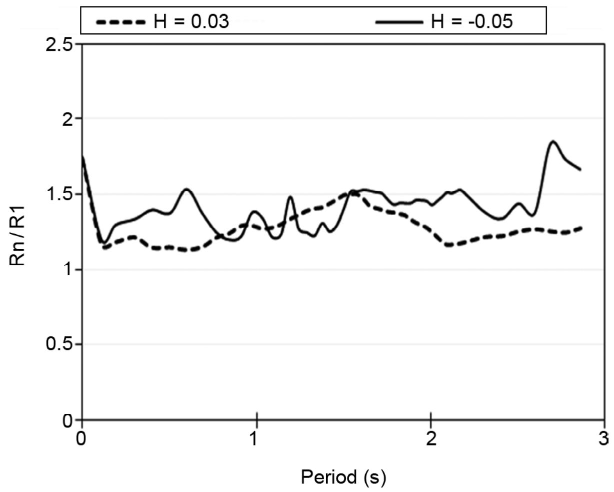

Figure 11. Effect of post-yield stiffness ratio of response spectrum at soil sites assuming μ = 8 and ξ = 5%.

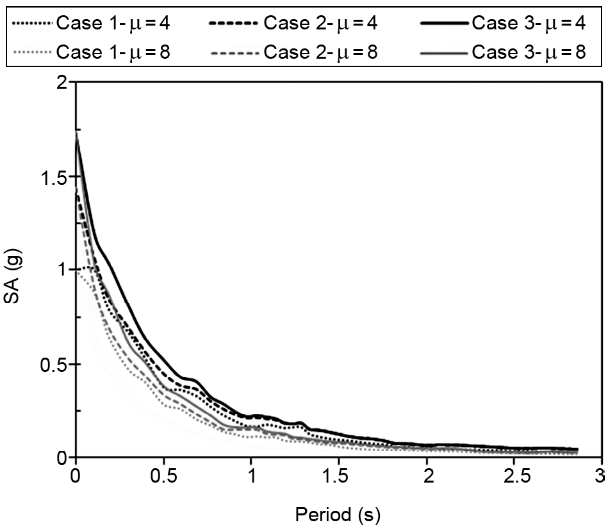

Figure 12. Effect of case ductility factors (μ = 4 and 8), ξ = 5%, and H = -0.03 on response spectrum at soil sites.

4.3. Effect of Ductility Ratio

The effect of ductility factor on response was investigated for different seismic sequences and the results are presented in Figures (14) and (15). The figures were plotted for post-yield stiffness ratios of 0.03 and -0.03, respectively, and compare the responses for case 1 and case 3. The responses were amplified in case 3 over case 1 as the ductility factor increased for periods of 0.2 to 2 s.

4.4. Aftershock and Rock Site Conditions

The result of the response spectrum for rock sites assuming μ = 1 in SDOF systems reveals no

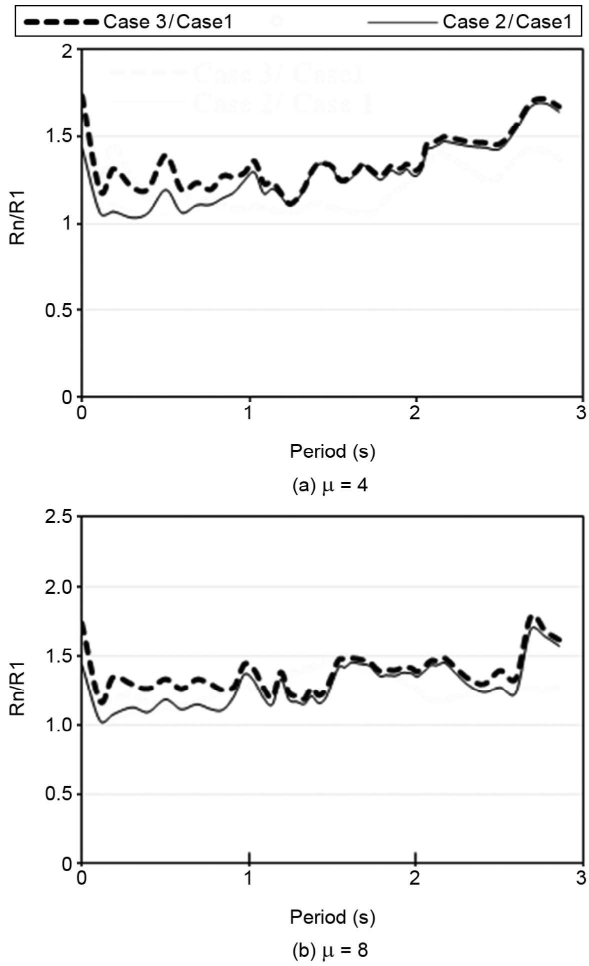

Figure 13. Effect of case and post-yield stiffness ratio of response spectrum at soil sites assuming H = -0.03 and ξ = 5%.

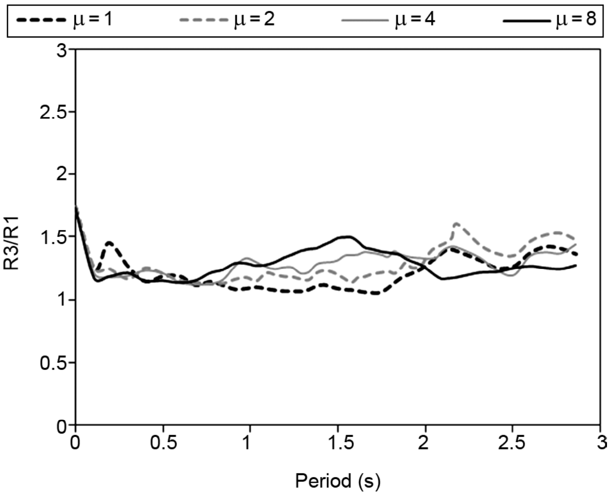

Figure 14. Effect of ductility factor (μ = 1, 2, 4 and 8) on response spectrum at soil sites for H = +0.03.

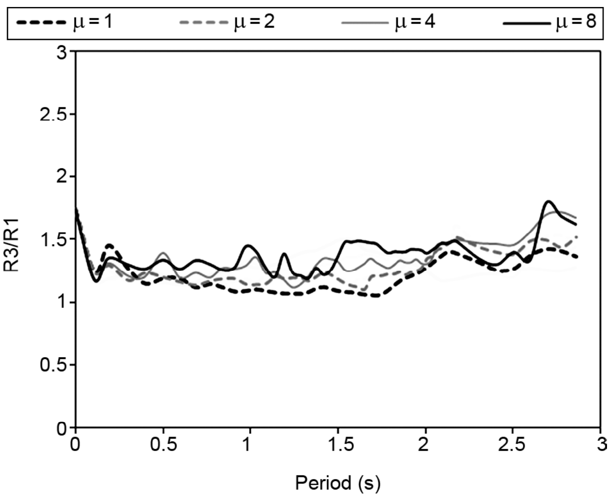

Figure 15. Effect of ductility factor (μ = 1, 2, 4 and 8) on response spectrum at soil sites for H = -0.03.

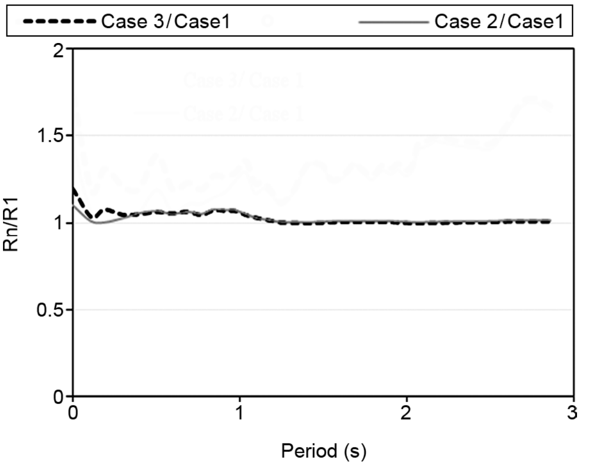

Figure 16. . Effect of case on response spectrum at rock sites assuming μ = 1, ξ = 5%, and H = 0.03.

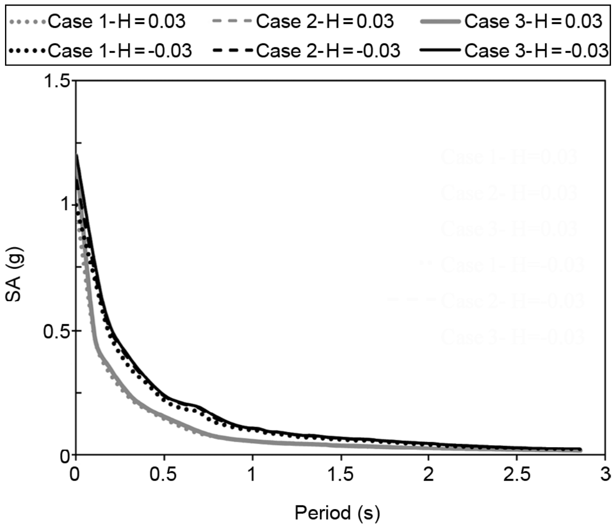

Figure 17. Effect of case on response spectrum at rock sites assuming μ = 8 and ξ = 5%.

significant changes under different seismic sequences (cases 1, 2, and 3). The ratio of spectral responses in case 3 over case 1 did not exceed 3.5% (Figure 16). Different cases of multiple earthquakes at rock sites had a negligible effect on the response spectrum of the SDOF system, unlike at soil sites. These results were also applicable and valid for other ductility factors. Figure (17) shows no change in structural response for the case by μ = 8 and post-yield stiffness ratios of 0.03 and -0.03 at rock sites.

The results shown in Figures (7) to (17) indicate that differences in the various parameters (such as ductility and post-yield stiffness ratio) are important for periods of 0.1 to 1.5 s. For periods that are longer than 1.5 s, the differences can be ignored.

4.5. Foreshocks, Aftershocks (Cases 1, 4 and 5) and Soil Site Conditions

The effects of both aftershocks and foreshocks on SDOF systems are presented in Table A2 in Appendix A (six records from six earthquakes and 28 aftershocks and foreshocks). Figure (18) compares the seismic sequences from cases 1, 4 and 5 for μ = 1 assuming a post-yield stiffness ratio of 0.03 and indicates differences of up to two-fold. The peak response in case 1 occurred in a period of 0.2 s and increased from 2.32 to 2.71 (17%) for case 4 (foreshock and mainshock) and from 2.32 to 4.83 (100%) for case 5 (foreshock, mainshock, and aftershock)

The effect of cases were compared assuming μ = 8 in Figures (19) and (20). No remarkable difference was observed with respect to μ = 1.

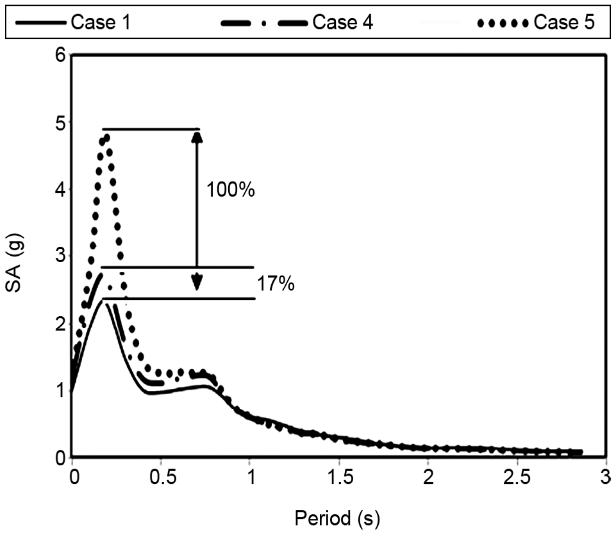

Figure 18. Effect of aftershock and foreshock on response spectrum for ductility factor 1, $\mu = 1$, $\xi = 5\%$, at soil sites.

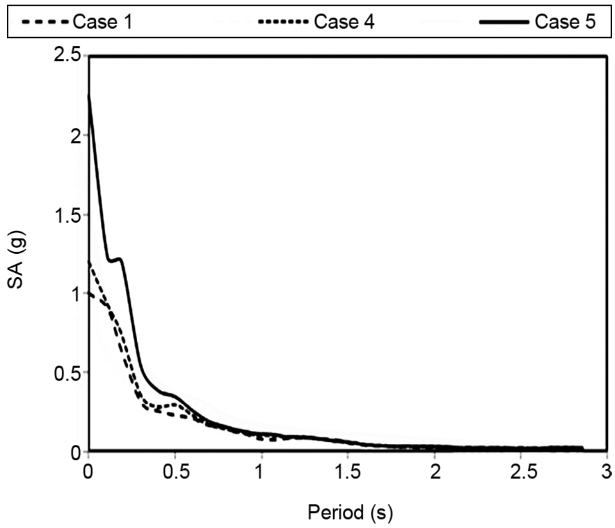

Figure 19. Effect of aftershock and foreshock on response spectrum for $\mu = 8$, $\xi = 5\%$, H = -0.03 for cases 1, 4 and 5.

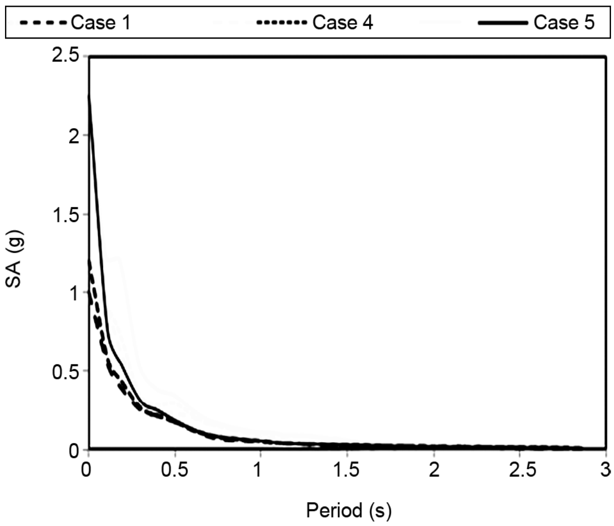

Figure 20. Effect of aftershock and foreshock on response spectrum for $\mu = 8$, $\xi = 5\%$, H = 0.03 for cases 1, 4 and 5.

The largest difference was for the period of 0.2 s and was about 38% for a post-yield stiffness ratio of 0.03 and 89% for a post-yield stiffness ratio of -0.03 (case 5) for the same period when compared to case 1 (mainshock). The largest difference occurred in a period of 0.2 s and was about 10% for $\mu = 8$ for a post-yield stiffness ratio of 0.03 and 15% for a post-yield stiffness ratio of -0.03 (case 4) when compared to case 1 (mainshock).

5. Conclusion

The present study compares the effects of aftershocks and foreshocks on the response spectrum of SDOF systems. To understand these effects, the parameters of period of vibration, ductility factor, soil conditions, and post-yield stiffness ratio (hardening and softening) were carefully examined. The following conclusions were drawn about the effect of these parameters on SDOF system structures subjected to multiple earthquakes.

- An event with multiple earthquakes that includes a mainshock and aftershocks (case 3) has a greater effect on the response spectrum than an event with only a mainshock (case 1) or a mainshock with one aftershock (case 2). Aftershocks can cause significant changes in the response spectrum that result in higher spectral amplitudes than for case 1 with only a mainshock. The results suggest that the effects of aftershocks must be considered in seismic design provisions for the design of safe structures and prevention of the destructive effects of aftershocks.
- The post-yield stiffness ratio affects the response spectrum. For post-yield stiffness ratios of -0.03 and 0.03, changes in spectral amplitude at soil sites increased from 18.5% to 34%.
- Cases of repeated earthquake ground motion showed negligible effects at rock sites, but had a major effect on SDOF systems at soil sites.
- All differences in response spectrum were for periods of 0.1 to 1.5 s. This means that the differences were negligible for periods longer than 1.5 s. Moreover, the seismic sequences in cases 2 and 3 were similar to case 1 for long periods. The results were similar for the effects of post-yield stiffness ratio and ductility factor on response spectrum.
- An increase in ductility factor amplified the

nonlinear response spectrum in a SDOF system. In systems having high ductility factors, the effects of the mainshock-aftershock sequences were more significant than the models with low ductility factor.

- Foreshocks (cases 4 and 5) could affect the inelastic response and lead to a significant increase in the response spectrum.

6. Data and Resources

The ground motion records were obtained from Iran Strong Motion Network (ISMN) [25] (http://site.bhrc.ac.ir/portal/english/Home.aspx), NIED Strong-motion seismograph networks, Japan [26] (http://www.kyoshin.bosai.go.jp/) and PEER Ground Motion Database, USA [21] (http://ngawest2.berkeley.edu).

Acknowledgements

The authors appreciate the valuable feedback and insightful conversations on the manuscript's topic that Associate Professor A. Ansari from IIEES, Professor A. Yazdani from the University of Kurdistan, and Dr. M.R. Soghrat from IIEES provided.

References

1. Yeo, G.L. and Cornell, C.A. (2005) *Stochastic Characterization and Decision Bases under Time-Dependent Aftershock Risk in Performance-Based Earthquake Engineering*. Report NO. 149, Pacific Earthquake Engineering Research Center, University of California, Berkeley, CA.

2. Mahin, S.A. (1980) Effects of duration and aftershocks on inelastic design earthquakes. *Proceedings of the 7th World Conference on Earthquake Engineering*, Istanbul, Turkey, 677-680.

3. Sunasaka, Y. and Kiremidjian, A.S. (1993) *A Method for Structural Safety Evaluation under Mainshock-Aftershock Earthquake Sequences*. Report No. 105, Department of Civil and Environmental Engineering, Stanford University: Palo Alto, CA.

4. Aschheim, M. and Black, E. (1999) Effects of prior earthquake damage on response of simple stiffness-degrading structures. *Earthquake Spectra*, **15**(1), 1-24.

5. Gallagher, R.P., Reasenberg, P.A., and Poland, C.D. (1999) *Earthquake Aftershocks-Entering Damaged Buildings*. Funded by the U.S. Geological Survey as Part of the ATC-35 Research Utilization Project.

6. Amadio, C., Fragiacomo, M., and Rajgelj, S. (2003) The effects of repeated earthquake ground motions on the non-linear response of SDOF systems. *Earthquake Engineering and Structural Dynamics*, **32**(2), 291-308.

7. Fragiacomo, M., Amadio, C., and Macorini, L. (2004) Seismic response of steel frames under repeated earthquake ground motions. *Engineering Structures*, **26**(13), 2021-2035.

8. Luco, N., Bazzurro, P., and Cornell, C.A. (2004) Dynamic versus static computation of the residual capacity of a mainshock-damaged building to withstand an aftershock. *Proceedings of 13th World Conference on Earthquake Engineering*, Vancouver, B.C. Paper No. 2405.

9. Iancovici, M. and Georgiana, I. (2007) Evaluation of the inelastic demand of structures subjected to multiple ground motions. *Journal of Structural Engineering*, **4**(2), 143-154.

10. Maeda, M. and Kang, D.E. (2009) Post-earthquake damage evaluation of reinforced concrete buildings. *Journal of Advanced Concrete Technology*, **7**(3), 327-335.

11. Hatzigeorgiou, G.D. and Beskos, D.E. (2009) Inelastic displacement ratios for SDOF structures subjected to repeated earthquakes. *Engineering Structures*, **31**(11), 2744-2755.

12. Hatzigeorgiou, G.D. and Liolios, A.A. (2010) Nonlinear behaviour of RC frames under repeated strong ground motions. *Soil Dynamics and Earthquake Engineering*, **30**(10), 1010-1025.

13. Moustafa, A. and Takewaki, I. (2011) Response of nonlinear single degree of freedom structures to random acceleration sequences. *Engineering Structures*, **33**(15), 1251-1258.

14. Zhang, S., Wang, G., and Sa, W. (2013) Damage

evaluation of concrete gravity dams under mainshock-aftershock seismic sequences. *Soil Dynamics and Earthquake Engineering*, **50**, 16-27.

15. Zhai, C.H., Wei, W. ZhiQiang, C., Li, S., and Xie, L.L. (2013) Damage spectra for the mainshock-aftershock sequence-type ground motions. *Soil Dynamics and Earthquake Engineering*, **45**, 1-12.

16. Jeon, J.S. (2013) *Aftershock Vulnerability Assessment of Damaged Reinforced Concrete Buildings in California*. Ph.D. Thesis, Georgia Institute of Technology, USA.

17. Iervolino, I., Giorgio, M., and Chioccarelli, E. (2014) Closed-form aftershock reliability of damage-cumulating elastic perfectly-plastic systems. *Earthquake Engineering and Structural Dynamics*, **43**(6), 13-25.

18. Zhai, C.H., Wen, W.P., Li, S., Chen, Z.Q., Chang, Z., and Xie, L.L. (2014) The damage investigation of inelastic SDOF structure under the mainshock-aftershock sequence-type ground motion. *Soil Dynamics and Earthquake Engineering*, **59**(14), 30-41.

19. Raghunandan, M., Lie, A.B., and Luco, N. (2014) Aftershock collapse vulnerability assessment of reinforced concrete frame structure. *Earthquake Engineering and Structural Dynamics*, **44**(3), 419-439.

20. Abdollahzadeh, G.R., Mohammadgholipour, A., and Omranian, E. (2018) Seismic evaluation of steel moment frames under mainshock-aftershock sequence designed by elastic design and PBPD methods. *Journal of Earthquake Engineering*, **23**(2), DOI: 10.1080/13632469.2017.1387198.

21. PEER (1999) *Strong Motion Database*. Pacific Earthquake Engineering Research. University of California, Berkeley, CA. http://peer.Berkeley.edu/NGA.

22. IIEES. International Institute of Earthquake Engineering and Seismology. http://www.iiees.ac.ir.

23. Chopra, A. (2006) *Dynamics of Structures: Theory and Applications to Earthquake Engineering*. 3rd ed. Prentice Hall; New Jersey.

24. OPENSEES (1999) *Open System for Earthquake Engineering Simulation*. Pacific Earthquake Engineering Research (PEER), University of California, Berkeley, CA. http://opensees.berkeley.edu.

25. Iran Strong Motion Network (ISMN) (http://site.bhrc.ac.ir/portal/english/Home.aspx).

26. NIED strong-motion seismograph networks, Japan. K-NET homepage. http://www.kyoshin.bosai.go.jp/.

27. IBC (2006) *International Building Code*. International Code Council, Inc., USA.

28. Boore, D.M. and Joyner, W.B. (1982) The empirical prediction of ground motion. *Bulletin of Seismological Society of America*, **72**(6), 43-60.

29. Stewart, J.P., and Chiou, S.J. Bray, J.D., Graves, R.W., Somerville, P.G., and Abrahamson, N.A. (2001) Ground motion evaluation procedures for performance-based design, PEER 2001/09. Pacific Earthquake Engineering Research Center, University of California, Berkeley, CA.

30. Trifunace, M.D. and Badly, A.G. (1975) A study on the duration of strong earthquake ground motion. *Bulletin of Seismological Society of America*, **65**(3), 581-626.

Appendix A

Table A1. Characteristics of mainshocks and aftershocks.

Record	Event	Date	Time	M	PGA (g)	Fourier Amplitude (m/s)	Max. Frequency (Hz)	t5-95 (s)	t5-75 (s)	Site Class
Japan MYG005 Station	Mainshock	11 Aug 1996	3:12	5.9	0.442	2.286	0.73	27.35	4.94	Rock
	Aftershock	11 Aug 1996	3:54	5.4	0.304	1.727	0.63	16.21	3.46	Rock
	Aftershock	11 Aug 1996	5:26	4.3	0.096	0.324	11.68	7.79	3.06	Rock
	Aftershock	11 Aug 1996	20:48	4.8	0.258	0.795	11.49	5.63	1.69	Rock
	Aftershock	11 Aug 1996	20:52	4.6	0.186	0.579	10.51	5.06	1.85	Rock
	Aftershock	13 Aug 1996	11:13	5	0.622	2.502	9.27	3.98	1.85	Rock
	Aftershock	14 Aug 1996	7:52	4.2	0.172	0.451	9.19	6.85	1.64	Rock
Japan KGS005 Station	Mainshock	26 Mar 1997	17:31	6.3	0.492	1.815	3.94	5.16	2.60	Rock
	Aftershock	26 Mar 1997	17:39	4.7	0.158	0.245	12.21	5.30	2.40	Rock
	Aftershock	26 Mar 1997	18:05	4.5	0.192	0.491	12.61	3.97	0.71	Rock
	Aftershock	26 Mar 1997	18:30	4	0.215	0.255	14.18	1.62	0.24	Rock
	Aftershock	26 Mar 1997	19:45	3.7	0.120	0.186	11.44	1.64	0.34	Rock
	Aftershock	26 Mar 1997	22:24	4.4	0.150	0.549	7.70	2.82	1.10	Rock
	Aftershock	27 Mar 1997	5:19	3.9	0.177	0.226	11.73	1.31	0.57	Rock
Japan KGS005 Station	Mainshock	13 May 1997	14:38	6.2	0.872	3.689	1.56	3.85	2.91	Rock
	Aftershock	14 May 1997	8:32	4.7	0.164	0.412	1.64	4.51	1.00	Rock
	Aftershock	25 May 1997	6:11	4.4	0.239	0.324	7.80	1.48	0.39	Rock
Japan HKD133 Station	Mainshock	29 Mar 2000	17:22	4.1	0.126	0.343	7.64	3.59	1.47	Rock
	Aftershock	29 Mar 2000	20:01	3.6	0.149	0.265	9.56	2.56	0.32	Rock
	Aftershock	29 Mar 2000	21:23	3.5	0.128	0.235	8.26	3.05	0.55	Rock
	Aftershock	30 Mar 2000	1:26	3.5	0.143	0.461	8.48	2.51	0.89	Rock
	Aftershock	30 Mar 2000	2:54	4	0.154	0.677	8.62	3.19	1.75	Rock
Japan TKY010 Station	Mainshock	3 Aug 2000	22:18	6.2	0.126	0.549	1.36	6.73	2.41	Soil
	Aftershock	18 Aug 2000	22:51	3.4	0.189	0.491	16.58	65.98	1.67	Soil
	Aftershock	29 Aug 2000	11:00	4.9	0.282	0.942	1.69	5.38	2.36	Soil
	Aftershock	29 Aug 2000	11:13	3.6	0.327	0.363	9.51	2.49	0.54	Soil
	Aftershock	29 Aug 2000	12:08	4.3	0.260	0.500	9.58	5.36	1.47	Soil
Japan TTR008 Station	Mainshock	6 Oct 2000	13:30	7.3	0.442	5.278	0.92	18.03	4.53	Soil
	Aftershock	7 Oct 2000	12:03	4.2	0.101	0.255	4.68	3.67	1.35	Soil
	Aftershock	8 Oct 2000	20:51	5	0.106	0.697	1.02	7.55	3.23	Soil
	Aftershock	10 Oct 2000	21:58	4.4	0.103	0.334	2.17	6.68	1.81	Soil
Japan MYG011 Station	Mainshock	26 May 2003	18:24	7	1.201	7.926	6.96	20.57	9.95	Rock
	Aftershock	26 May 2003	22:34	4.8	0.119	0.363	7.25	7.89	1.26	Rock
	Aftershock	27 May 2003	0:44	4.9	0.229	0.657	8.50	5.36	0.90	Rock
	Aftershock	31 May 2003	18:42	4.7	0.109	0.245	12.64	11.44	3.84	Rock
	Aftershock	10 Jun 2003	16:24	4.9	0.126	0.618	6.00	12.55	1.37	Rock
Japan HKD100 Station	Aftershock	26 Sep 2003	6:08	7.1	0.450	4.454	4.82	33.77	21.96	Soil
	Aftershock	29 Sep 2003	11:37	6.5	0.102	1.128	4.79	12.61	5.58	Soil
Japan NIG020 Station	Mainshock	23 Oct 2004	17:56	6.8	0.599	3.541	4.12	69.01	6.61	Rock
	Aftershock	23 Oct 2004	18:03	-	0.280	2.668	3.81	6.77	2.76	Rock
	Aftershock	23 Oct 2004	18:07	5.7	0.131	0.569	8.16	152.7	31.18	Rock
	Aftershock	23 Oct 2004	18:12	6	0.269	1.148	3.97	13.15	1.62	Rock
	Aftershock	23 Oct 2004	8:09	6.5	0.572	3.669	3.78	122.3	3.78	Rock
	Aftershock	23 Oct 2004	19:46	5.7	0.156	1.001	7.40	209.5	159.0	Rock
	Aftershock	23 Oct 2004	23:34	5.3	0.255	0.608	3.35	3.06	1.52	Rock
	Aftershock	23 Oct 2004	6:05	5.8	0.440	1.560	4.14	8.48	1.52	Rock
	Aftershock	23 Oct 2004	10:40	6.1	0.534	1.933	3.12	20.81	2.23	Rock
Japan SZO002 Station	Mainshock	21 Apr 2006	2:50	5.8	0.376	1.295	3.27	4.39	1.21	Soil
	Aftershock	21 Apr 2006	3:20	4.5	0.153	0.549	3.41	1.68	0.59	Soil
	Aftershock	21 Apr 2006	23:17	4.5	0.154	0.726	3.41	1.60	0.71	Soil
	Aftershock	2 May 2006	18:24	5.1	0.229	0.755	2.76	1.61	0.55	Soil
Japan ISK003 Station	Mainshock	25 Mar 2007	9:42	6.9	0.512	2.560	1.16	10.35	3.19	Rock
	Aftershock	25 Mar 2007	18:11	5.3	0.268	0.726	1.60	3.16	1.03	Rock
	Aftershock	28 Mar 2007	8:08	4.9	0.129	0.314	3.96	2.84	0.46	Rock
Japan NIG018 Station	Mainshock	16 Jul 2007	10:13	6.8	0.633	7.691	0.43	7.08	5.78	Soil
	Aftershock	16 Jul 2007	15:37	5.8	0.202	0.677	7.70	7.78	2.73	Soil
	Aftershock	16 Jul 2007	18:19	4.4	0.115	0.245	9.77	2.75	1.12	Soil

Table A1. Continue.

Record	Event	Date	Time	M	PGA (g)	Fourier Amplitude (m/s)	Max. Frequency (Hz)	t5-95 (s)	t5-75 (s)	Site Class
Japan MYG005 Station	Mainshock	14 Jun 2008	8:43	7.2	0.501	5.376	0.66	39.21	8.41	Rock
	Aftershock	14 Jun 2008	8:52	4	0.180	1.089	10.82	242.0	240.6	Rock
	Aftershock	14 Jun 2008	8:58	3.8	0.261	0.677	10.38	2.51	0.94	Rock
	Aftershock	14 Jun 2008	8:59	3.6	0.103	0.500	10.34	109.2	39.26	Rock
	Aftershock	14 Jun 2008	9:14	3.5	0.133	0.392	10.46	74.89	72.64	Rock
	Aftershock	14 Jun 2008	9:20	5.7	0.273	1.530	0.54	21.82	3.32	Rock
Japan-FKS025 Station	Mainshock	29 Sep 2010	17:00	5.7	0.210	0.785	11.51	43.89	3.17	Rock
	Aftershock	30 Sep 2010	20:05	3.6	0.150	0.265	12.93	0.84	0.38	Rock
	Aftershock	1 Oct 2010	8:24	4.4	0.079	0.177	8.28	1.39	0.47	Rock
Japan-MYG004 Station	Mainshock	11 Mar 2011	14:46	9	3.120	26.821	6.00	80.86	52.16	Rock
	Aftershock	11 Mar 2011	15:09	7.4	0.112	0.961	6.33	218.3	179.0	Rock
	Aftershock	11 Mar 2011	15:26	7.5	0.096	1.167	7.86	46.65	31.12	Rock
	Aftershock	11 Mar 2011	16:29	6.5	0.240	1.697	6.07	24.18	16.14	Rock
	Aftershock	11 Mar 2011	20:37	6.7	0.109	0.903	7.68	160.9	13.56	Rock
	Aftershock	24 Mar 2011	17:21	6.2	0.176	0.912	6.47	12.20	3.46	Rock
	Aftershock	28 Mar 2011	7:24	6.5	0.122	0.657	6.23	22.93	8.77	Rock
	Aftershock	2 Apr 2011	13:08	5.2	0.125	0.481	8.81	7.38	2.11	Rock
	Aftershock	7 Apr 2011	23:32	7.1	1.211	11.085	6.00	15.75	7.67	Rock
	Aftershock	9 Apr 2011	18:42	5.4	0.187	0.863	9.48	4.91	1.01	Rock
Coalinga-Sulphur Baths Station	Mainshock	22 Jul 1983	2:39	5.8	0.140	0.500	5.26	9.66	2.15	Rock
	Aftershock	25 Jul 1983	22:31	5.2	0.150	0.353	2.27	5.24	1.04	Rock
Hollister-Hollister 1028 Station	Mainshock	9 Apr 1961	7:23	5.6	0.200	0.961	2.38	16.52	7.67	Soil
	Aftershock	9 Apr 1961	7:25	5.5	0.080	0.785	1.64	15.92	7.55	Soil
Imperial Valley-Bonds Corner Station	Mainshock	15 Oct 1979	23:16	6.5	0.770	5.023	1.59	9.75	4.66	Soil
	Aftershock	15 Oct 1979	23:19	5.0	0.100	0.402	1.41	9.66	1.59	Soil
Irpinia Italy-Marcato Station	Mainshock	23 Nov 1980	19:34	6.9	0.150	1.687	1.15	25.23	11.21	Soil
	Aftershock	23 Nov 1980	19:35	6.2	0.040	0.598	1.35	17.94	8.93	Soil
Irpinia Italy-Sturno Station	Mainshock	23 Nov 1980	19:34	6.9	0.360	2.590	0.43	15.5	6.33	Rock
	Aftershock	23 Nov 1980	19:35	6.2	0.080	0.530	1.79	14.12	5.03	Rock
Livermol-Apeel 58219 Station	Mainshock	24 Jan 1980	19:00	5.8	0.070	0.304	3.13	7.73	2.55	Rock
	Aftershock	27 Jan 1980	2:33	5.4	0.050	0.196	3.03	6.39	1.16	Rock
Mamooth Lakes-Convict Creek Station	Mainshock	25 May 1980	16:34	6.1	0.442	2.619	1.47	9.34	7.14	Soil
	Aftershock	25 May 1980	16:49	5.7	0.160	0.863	3.13	7.43	2.58	Soil
	Aftershock	25 May 1980	19:44	5.9	0.220	0.952	1.79	6.31	2.76	Soil
	Aftershock	25 May 1980	20:35	5.7	0.380	1.167	3.33	3.76	2.64	Soil
	Aftershock	26 May 1980	18:58	5.7	0.130	0.373	1.75	5.54	1.70	Soil
	Aftershock	27 May 1980	14:51	5.9	0.270	0.991	1.96	6.81	2.83	Soil
Mamooth Lakes-Convict Creek Station	Mainshock	7 Jan 1983	1:38	5.3	0.170	1.040	1.64	7.18	2.81	Soil
	Aftershock	7 Jan 1983	3:24	5.3	0.150	0.569	1.35	7.12	2.01	Soil
Superstitn Hills-Wild Life 5210 Station	Mainshock	24 Nov 1987	5:14	6.2	0.130	0.824	2.78	15.34	7.10	Soil
	Aftershock	24 Nov 1987	13:16	6.5	0.180	2.040	0.38	33.96	19.61	Soil
Iran-Ab Bar Station	Mainshock	20 Jun 1990	21:00	6.4	0.560	3.630	4.58	30.65	11.77	Rock
	Aftershock	21 Jun 1990	9:02	5.8	0.132	0.324	8.40	4.33	3.04	Rock
	Aftershock	21 Jun 1990	21:27	4.9	0.066	0.177	8.89	2.87	1.63	Rock
	Aftershock	24 Jun 1990	9:46	5.1	0.057	0.078	4.69	5.45	4.40	Rock
	Aftershock	1 Jul 1990	17:19	4.6	0.065	0.098	3.98	5.52	3.07	Rock
	Aftershock	6 Jul 1990	19:34	5.3	0.066	0.147	1.42	4.46	0.67	Rock
Iran-Tabas Station	Mainshock	16 Sep 1978	15:35	6.4	0.960	5.494	1.26	19.13	8.67	Rock
	Aftershock	16 Sep 1978	16:53	4.4	0.140	0.029	7.14	6.50	0.95	Rock
	Aftershock	16 Sep 1978	18:25	4.7	0.107	0.226	7.62	3.85	1.36	Rock
	Aftershock	16 Sep 1978	18:45	4.8	0.068	0.196	5.22	7.90	2.60	Rock
	Aftershock	16 Sep 1978	20:30	4.3	0.058	0.304	3.12	20.22	17.75	Rock
	Aftershock	17 Sep 1978	7:35	4.5	0.172	0.402	2.05	4.19	2.50	Rock
	Aftershock	18 Sep 1978	4:50	4.7	0.053	0.078	5.17	5.40	1.64	Rock
	Aftershock	18 Sep 1978	17:35	4.9	0.114	0.216	6.79	5.44	1.38	Rock
	Aftershock	19 Sep 1978	1:49	4.7	0.162	0.314	3.81	2.78	0.63	Rock
Iran-Meymand Station	Mainshock	20 Jun 1994	9:09	5.9	0.483	1.687	4.27	6.07	2.10	Rock
	Aftershock	21 Jun 1994	4:15	4.7	0.146	1.236	0.73	9.16	4.41	Rock
Iran-Hosseiniyeh Olya Station	Mainshock	31 Jul 1994	6:15	5.3	0.186	0.520	1.95	6.57	1.95	Rock
	Aftershock	31 Jul 1994	5:22	5.2	0.183	0.491	1.90	3.96	0.42	Rock

Table A1. Continue.

Record	Event	Date	Time	M	PGA (g)	Fourier Amplitude (m/s)	Max. Frequency (Hz)	t5-95 (s)	t5-75 (s)	Site Class
Iran-Sirch Station	Mainshock	14 Mar 1998	19:40	5.9	0.584	3.227	0.85	6.32	5.00	Rock
	Aftershock	16 Mar 1998	4:16	4.1	0.089	0.216	3.61	3.00	0.68	Rock
	Aftershock	16 Mar 1998	20:29	3.9	0.090	0.088	5.86	1.05	0.11	Rock
	Aftershock	17 Mar 1998	4:53	3.5	0.054	0.069	6.25	2.75	0.50	Rock
Iran-Golbaf Station	Mainshock	July 28, 1981	17:22	5.9	0.293	2.796	0.65	37.90	17.92	Rock
	Aftershock	July 28, 1981	18:04	4.6	0.050	0.029	5.57	5.41	1.48	Rock
	Aftershock	July 28, 1981	21:54	4.9	0.057	0.128	3.12	2.35	0.61	Rock
	Aftershock	July 30, 1981	5:20	3.9	0.076	0.118	4.00	2.46	0.96	Rock
	Aftershock	July 30, 1981	11:14	4.2	0.055	0.098	4.78	2.08	0.57	Rock
	Aftershock	July 31, 1981	0:37	4.5	0.110	0.118	3.22	2.83	1.20	Rock
	Aftershock	3 Aug 1981	2:55	4.6	0.182	0.167	3.37	0.94	0.13	Rock
	Aftershock	8 Aug 1981	4:17	4.8	0.097	0.235	3.51	3.14	0.51	Rock
Iran-Garmsar Station	Mainshock	24 Oct 1988	17:01	4.9	0.111	0.245	7.57	5.11	2.23	Rock
	Aftershock	26 Oct 1988	14:49	4.7	0.057	0.235	6.44	6.34	3.10	Rock
	Aftershock	3 Dec 1988	18:41	4.4	0.140	0.432	5.91	2.35	0.48	Rock
Iran-Abgarm Station	Mainshock	22 Jun 2002	2:58		0.126	2.335	2.33	15.16	71.00	Soil
	Aftershock	22 Jun 2002	6:45		0.075	0.785	2.44	10.46	5.17	Soil

Table A2. Characteristics of mainshocks, aftershocks and foreshocks.

Record	Event	Date	Time	M	PGA (g)	Fourier Amplitude (m/s)	Max. Frequency (Hz)	t5-95 (s)	t5-75 (s)	Site Class
Japan-SZO002 Station	Foreshock	3 Mar 1997	14:20	4	0.124	0.510	3.48	1.34	0.71	Soil
	Foreshock	3 Mar 1997	20:11	4.5	0.161	0.392	2.70	2.19	1.01	Soil
	Foreshock	3 Mar 1997	23:09	5	0.522	3.247	2.58	3.05	1.40	Soil
	Foreshock	4 Mar 1997	0:03	4.9	0.345	1.256	2.57	1.79	0.62	Soil
	Mainshock	4 Mar 1997	12:51	5.7	0.158	1.256	3.26	4.92	2.76	Soil
	Aftershock	5 Mar 1997	22:43	4.4	0.296	1.167	3.16	1.09	0.71	Soil
	Aftershock	7 Mar 1997	2:36	4	0.210	0.540	2.83	1.75	0.96	Soil
	Aftershock	7 Mar 1997	16:33	4.6	0.294	0.971	3.19	3.84	1.65	Soil
Japan-MYG010 Station	Foreshock	26 Jul 2003	0:13	5.5	0.149	0.932	0.99	15.25	4.57	Soil
	Mainshock	26 Jul 2003	7:13	6.2	0.210	1.599	0.77	17.25	4.75	Soil
	Aftershock	28 Jul 2003	4:08	5	0.147	0.598	0.95	11.71	5.38	Soil
Japan-HKD100 Station	Foreshock	27 Nov 2004	7:42	5.6	0.140	0.952	6.14	10.87	5.55	Soil
	Mainshock	29 Nov 2004	3:32	7.1	0.140	1.128	5.43	14.25	6.18	Soil
	Aftershock	6 Dec 2004	23:15	6.9	0.100	0.755	4.86	14.03	6.07	Soil
Japan-SZO002 Station	Foreshock	17 Dec 2009	23:45	5	0.475	2.423	2.36	1.84	1.05	Soil
	Foreshock	18 Dec 2009	0:40	3.5	0.132	0.343	2.86	2.08	1.20	Soil
	Foreshock	18 Dec 2009	2:30	4.2	0.125	0.343	3.42	1.84	0.93	Soil
	Foreshock	18 Dec 2009	5:25	4	0.144	0.284	3.06	3.11	1.57	Soil
	Mainshock	18 Dec 2009	8:45	5.1	0.737	2.649	2.38	1.55	0.70	Soil
	Aftershock	18 Dec 2009	16:39	3.9	0.105	0.383	2.80	2.42	1.38	Soil
	Aftershock	18 Dec 2009	21:27	3.9	0.162	0.726	2.70	1.44	0.59	Soil
	Aftershock	19 Dec 2009	0:53	4.5	0.346	0.893	2.71	1.88	1.51	Soil
	Aftershock	19 Dec 2009	1:52	3.7	0.112	0.343	2.78	2.16	1.64	Soil
	Aftershock	19 Dec 2009	3:36	3.6	0.142	0.383	3.06	1.86	1.43	Soil
	Aftershock	19 Dec 2009	18:11	3.9	0.173	0.647	2.65	2.34	1.56	Soil
	Aftershock	19 Dec 2009	22:04	4.3	0.205	0.765	3.19	1.87	1.19	Soil
	Aftershock	19 Dec 2009	22:09	4.5	0.176	0.795	2.65	1.48	0.88	Soil
Chalfant Valley Beshop 54171 Station	Foreshock	20 Jul 1986	14:29	5.8	0.129	1.265	0.91	20.23	8.5	Soil
	Mainshock	21 Jul 1986	14:42	6.2	0.248	1.246	0.85	12.57	3.6	Soil
	Aftershock	21 Jul 1986	14:51	5.7	0.110	0.412	4.35	13.85	2.17	Soil
Chalfant Valley-Zack Brothers Station	Foreshock	20 Jul 1986	14:29	5.8	0.210	1.540	2.17	11.48	3.08	Soil
	Mainshock	21 Jul 1986	14:42	6.2	0.400	3.463	1.32	8.12	2.58	Soil
	Aftershock	21 Jul 1986	14:51	5.7	0.110	0.402	9.09	10.94	3.6	Soil